The application of parametric estimation techniques to wavelength scanning interferometry

REBECCA LUCY WOODCOCK

The University of Huddersfield

August 2017

Copyright Statement

ABSTRACT

The growth in the manufacture of complex surfaces means that surface metrology has become an essential part of the manufacturing process in many industries. Wavelength scanning interferometry (WSI) is a technique that enables fast surface topography measurement. Since WSI can be implemented without the measurand or apparatus being mechanically moved, the measurement times are substantially less than other topography techniques that require mechanical movement. A variety of algorithms can be used to evaluate the spectral interferograms generated from WSI, and the choice of algorithm affects the axial (height) resolution and measurement range that can be attained. At present Fourier transform based methods are the most commonly used, but these can have a number of limitations, including problems which derive from short data lengths.

In order to extend the measurement range of the WSI, frequency estimation techniques based on an auto-regressive model are introduced. In particular, the Burg method is suggested as an alternative to current algorithms and a comparison is made to Fourier-transform methods using both simulated data and experimental data of a step-height sample measured using WSI.

List of Contents

List of Figures

List of Tables

1. Introduction

1.1. Overview

Components with complex structured and freeform surfaces are a vital part of modern industries. To ensure these components function as desired it is necessary to be able to accurately measure and characterise their surface.

The metrology techniques used for different applications are dependent on the measurement environment as well as the surface being measured. Contact-based stylus methods are popular due to the range to resolution ratio but non-contact methods are preferred where a stylus would be destructive to the surface. Interferometry provides a non-contact method surface metrology technique that can characterise surfaces with a fast response time and without causing damage.

Various types of interferometer can be used for surface metrology. Currently scanning white light interferometry (SWLI) is the most commonly used technique in industry. However, wavelength scanning interferometry (WSI) is an alternative with a faster measurement speed, as it does not require mechanical scanning.

WSI generates a set of sinusoidal intensity patterns which each correspond to a point of the surface being measured. To determine the height of the surface at a particular point, the phase shift that occurs during the wavelength scan is calculated. At present Fourier techniques are most commonly used to calculate the phase shift. Parametric methods are an alternative approach which can potentially provide better results where the data length is short.

1.2. Aim

The aim of this research is to develop a parametric phase estimation algorithm that can be used to calculate the height of a surface measured using WSI. The algorithm should be able to extend the measurement range of the WSI compared to current Fourier techniques.

1.3. Objectives

The objectives of this work are as follows:

- Develop a method to apply parametric estimation techniques to wavelength scanning interferometer output.
- Test the efficacy of parametric algorithms on data simulated interferometer output.
- Conduct a comparison study between parametric and Fourier estimation methods using real data collected for the WSI.

1.4. Contribution

The work contained in this thesis makes the following novel contribution to knowledge:

- The introduction of parametric estimation methods to calculate the surface height from WSI output.
- The demonstration of WSI surface analysis using the Burg algorithm and a tapered form of the Burg algorithm.
- The introduction of a comparison study to evaluate the performance of the Burg methods of height estimation in relation to Fourier methods.
- Knowledge transfer through the publication of research into algorithms for WSI.

1.5. Thesis Layout

The thesis is structured as follows:

- Chapter 2 gives an overview of surface metrology with specific reference to wavelength scanning interferometry. A description of the method for calculating the surface height from the WSI output is given.
- Chapter 3 discusses algorithms for determining the surface height from the WSI output. A comparison between the Burg methods and current Fourier techniques is given.
- Chapter 4 gives an overview of the application of the Burg algorithm to WSI as well as conclusions and proposals for future work.

2. Wavelength scanning interferometry

2.1. Introduction

This chapter describes the characteristics of wavelength scanning interferometry and how the surface height can be calculated from the interferometer output.

2.2. Surface metrology

The emergence of nanotechnology and ultra-precision surfaces has caused a paradigm shift in surface metrology. Surface measurement is of vital importance to precision engineering and should be able to be applied to complex freeform and structured surfaces. Techniques are required that can provide an areal characterisation of these complex surfaces.

Surface metrology is the science of measuring small-scale geometrical features on surfaces (Jiang et al, 2007). These features can be divided into roughness (short wavelength component), waviness (longer wavelength component) and form (very long wavelength component).

A wide range of measurement principles are used in established laboratory-based surface metrology instruments. Currently stylus profilometers provide the best vertical range versus resolution, but the lateral resolution depends of the stylus radius. Reducing the radius increases the likelihood of the surface being damaged by scratching.

A variety of optical techniques are also well established. These have the advantage of being non-destructive and relatively fast. Interferometers that measure the phase shift of light reflected from a surface can be used to characterise surfaces. However when a single wavelength is used there is a problem of 2π phase ambiguity. This occurs because

for one wavelength the phase difference can only be calculated modulo 2π and so surfaces separated by an integer multiple of the wavelength cannot be distinguished. While optically smooth surfaces can be measured with this technique, difficulties occur with rough and structured surface. There are various ways to overcome the 2π phase ambiguity problem.

Currently, scanning white light interferometry (SWLI) is the most common optical technique used in industry. A white light source is used and the interferogram produced is a superposition of the fringe patterns created from each wavelength. If two different heights have the same fringe pattern from one wavelength, they can still be distinguished using the other wavelength components of the white light. At the centre of the interferogram the optical path difference will be zero for every wavelength, producing a white fringe. Moving away from the centre there will be a sequence of interference colours as the spacing of the fringes will be different for each wavelength. In an SWLI system the interferometer objective is scanned vertically and the variance of the interference as a function of the optical path difference is recorded. The surface height at each point can then be calculated from this information.

SWLI instruments can characterise surfaces with nanometre uncertainty over 200 μm vertical range. However the technique can be slow if a large vertical measurement range is required because of the need to physically move the objective or sample through the range. The measurement speed as well as the size and complexity of the SWLI instruments mean that they are usually restricted to laboratory environments. New optical techniques are being developed with the aim of providing fast measurement in manufacturing environments.

2.2.1. State of the art

Currently, scanning white light interferometry (SWLI) is the most common optical technique used in industry. A white light source is used and the interferogram produced is a superposition of the fringe patterns created from each wavelength. If two different heights have the same fringe pattern from one wavelength, they can still be distinguished using the other wavelength components of the white light. At the centre of the interferogram the optical path difference will be zero for every wavelength, producing a white fringe. Moving away from the centre there will be a sequence of interference colours as the spacing of the fringes will be different for each wavelength. In an SWLI system the interferometer objective is scanned vertically and the variance of the interference as a function of the optical path difference is recorded. The surface height at each point can then be calculated from this information.

SWLI instruments can characterise surfaces with nanometre uncertainty over a vertical range of 200 μm. However, the technique can be slow if a large vertical measurement range is required because of the need to physically move the objective or sample through the range. The measurement speed as well as the size and complexity of the SWLI instruments mean that they are usually restricted to laboratory environments. New optical techniques are being developed with the aim of providing fast measurement in manufacturing environments.

Wavelength scanning interferometry uses a light source that can be tuned to a particular wavelength. The tuneable wavelength can be provided by a tuneable laser or by a white light source passed through an acousto-optic tuneable filter. Different wavelengths of light pass through the interferometer and produce a series of interferograms from which the optical path difference can be calculated. Kikuta et al. (1986) first demonstrated

distance measurement using injection current driven wavelength scanning in diode lasers. Kuwamura and Yamaguchi (1997) used a tuneable dye laser to extend the wavelength scanning range of WSI for surface profilometry and were able to achieve an axial resolution of a few tens of nanometres. A variation of WSI creates wavelength scanning using an acousto-optic tuneable filter combined with a halogen source (Jiang et al, 2010). This can achieve a large wavelength scanning range, and thus good axial resolution, at relatively low cost. WSI has advantages over SWLI as it does not require any mechanical movement of the probe or specimen and processing the data is simpler and quicker.

One important application for WSI relates to roll-to-roll processing. The manufacture of roll-to-roll coated polymer film requires an online inspection system to optimise the process, as nano-scale defects in the films have been shown to negatively impact their performance. The inspection system needs to be fast and non-contact, and be able to function in a “noisy” environment. WSI is capable of meeting these requirements.

Wavelength dispersive interferometry uses a dispersive optical element which causes different wavelengths of light to travel different optical paths. Each wavelength is then used to measure the surface at a height which causes zero optical path difference in the reference and measurement arms. One type of dispersive element that can be used is a blazed grating.

2.2. WSI principle of operation

The wavelength scanning interferometer works by measuring the phase shift of light reflected from a surface. The configuration of the measurement system is shown in Figure 2.1. A white light source is used, and is passed through an acousto-optic tuneable filter

(AOTF) so that the wavelengths required for the interferograms can be selected. The AOTF uses a birefringent crystal which transmits a single wavelength of light which can be varied by applying an acoustic wave. The wavelength is tuned from 683.42 nm to 590.98 nm.

There is also a reference interferometer illuminated by a near-infrared superluminescent light-emitting diode (SLED) which shares the same optical path. The SLED has a wavelength of 816.2 nm and a bandwidth of 25 nm filtered to 3 nm. This is used to compensate for environmental noise. A piezoelectric translator is attached to the reference mirror, moving it to create a change in optical path length that cancels out the change in optical path length created by environmental noise caused by out of plane vibration of the surface. Since the measurement and reference interferometers share the same optical path this should eliminate most noise from the measurement.

After passing through the AOTF the light is combined with the light from the SLED using a dichroic beam splitter and is transmitted to the interferometer by an optical fibre. The Linnik configuration sends part of the light to the reference mirror and part to the sample and then recombines it to create an interferogram. The Linnik configuration compensates for aberrations such as chromatic dispersion.

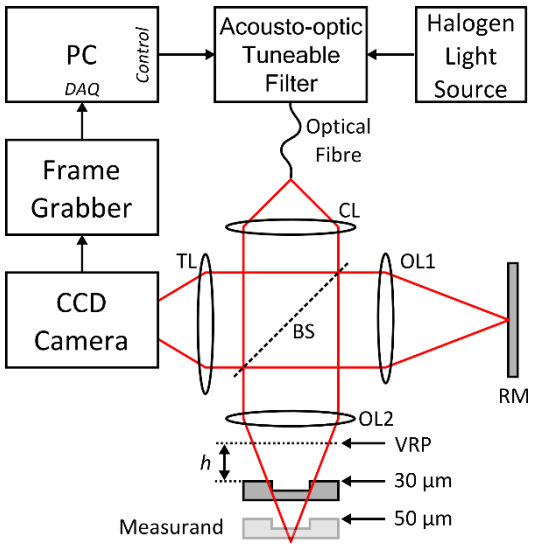

Fig. 2.1. The configuration of the wavelength scanning interferometer.

2.2.1. Calculating the surface height from the interferometer output

WSI generates a set of spectral interferograms, where each pixel corresponds to a point of the surface being measured. At each pixel a sinusoidal intensity pattern is recorded, caused by the scanning of the wavelength during measurement. To determine the surface height at each point, the phase shift that occurs during the wavelength scan needs to be calculated. The wavelength of light transmitted by the AOTF is given by the equation

$$\lambda = \alpha \Delta n \frac{v_a}{f_a} \tag{2.1}$$

where α is a constant depending on the AOTF design, Δn is the birefringence of the crystal and v_a and f_a are the propagation velocity and frequency of the acoustic wave.

Since Δn can be assumed to be constant the equation shows that if the frequency of the acoustic wave is changed linearly the reciprocal of the transmitted wavelength will also change linearly. This means that there will be a linear phase shift in the interference pattern. The output of the WSI is detected by a CCD camera with each pixel of the CCD corresponding to a point of the surface being measured. Across all captured frames a pixel at position (x, y) will show a sinusoidal intensity distribution that can be expressed in terms of the fringe visibility $a_{xy}(\lambda)$ and the background intensity $b_{xy}(\lambda)$ as

$$I_{xy}(\lambda) = a_{xy}(\lambda)\cos\left(\phi_{xy}(\lambda)\right) + b_{xy}(\lambda) \tag{2.2}$$

where λ is the wavelength and ϕ is the phase of the interference signal. The phase shift caused by a certain change in wavelength is given by

$$\Delta\phi_{xy}(\lambda) = \frac{2\pi}{\lambda_s} h_{xy} \tag{2.3}$$

where λ_s is the synthetic wavelength ($\lambda_{max}\lambda_{min}/\lambda_{max} - \lambda_{min}$) and h_{xy} is the optical path difference. Thus the height of the surface at each point can be determined by finding the phase change across the wavelength scanning range.

Various different types of algorithm can be used to calculate the phase shift that occurs due to wavelength scanning. The algorithm chosen is one of the factors that affects the resolution of the surface height measurement from WSI. The more accurate the determination of the phase shift, the higher the resolution that can be obtained. At present, Fourier transform methods are the most common phase estimation technique.

One easy way to evaluate the phase shift caused by wavelength scanning is to use a fast Fourier transform (FFT). The FFT generates a power spectral density (PSD) corresponding to the interference pattern. The peak of the PSD function is the number of the cycles in the sinusoidal pattern produced by wavelength scanning. However this method has a low resolution, limited to $\lambda_s/2$, where λ_s is the synthetic wavelength of the light source. This corresponds to an axial resolution which is at best in the micron scale when the wavelength of the scanned light is in the visible. The resolution of the FFT method can be improved to some degree by using curve fitting on the spectrum before finding the Fourier peak, in order to allow the phase to be estimated within the 2π interval.

A technique to further improve the FFT results by determining the rate of change of instantaneous phase during wavelength scanning was developed by Takeda et al. (1994). In WSI, the wavenumber of the light source is changed linearly, which means that the change in phase will also be linear. The optical path difference at each pixel can be calculated by finding the rate of change of phase as the wavelength is scanned. Using this technique eliminates the problems associated with identifying the peak of a PSD and can provide better height resolution in comparison to the simple FFT method. Figure 2.2 shows how the Takeda technique is applied. The interference pattern is first processed by FFT to separate the exponential term of the phase from the unwanted terms such as light bias, noise and the conjugate term of the phase. After filtering out the unwanted terms, the inverse FFT is applied to retrieve the exponential term of the phase. The wrapped phase can be extracted from the exponential form simply by using the natural logarithm. This can then be corrected by adding a phase set distribution, hence constructing the unwrapped phase. However, since this method relies on phase unwrapping, an reduction in the number of data points per cycle of the interference pattern causes the resolution to decrease. For shorter data records it may be advantageous to use a non-Fourier method to get improved frequency resolution.

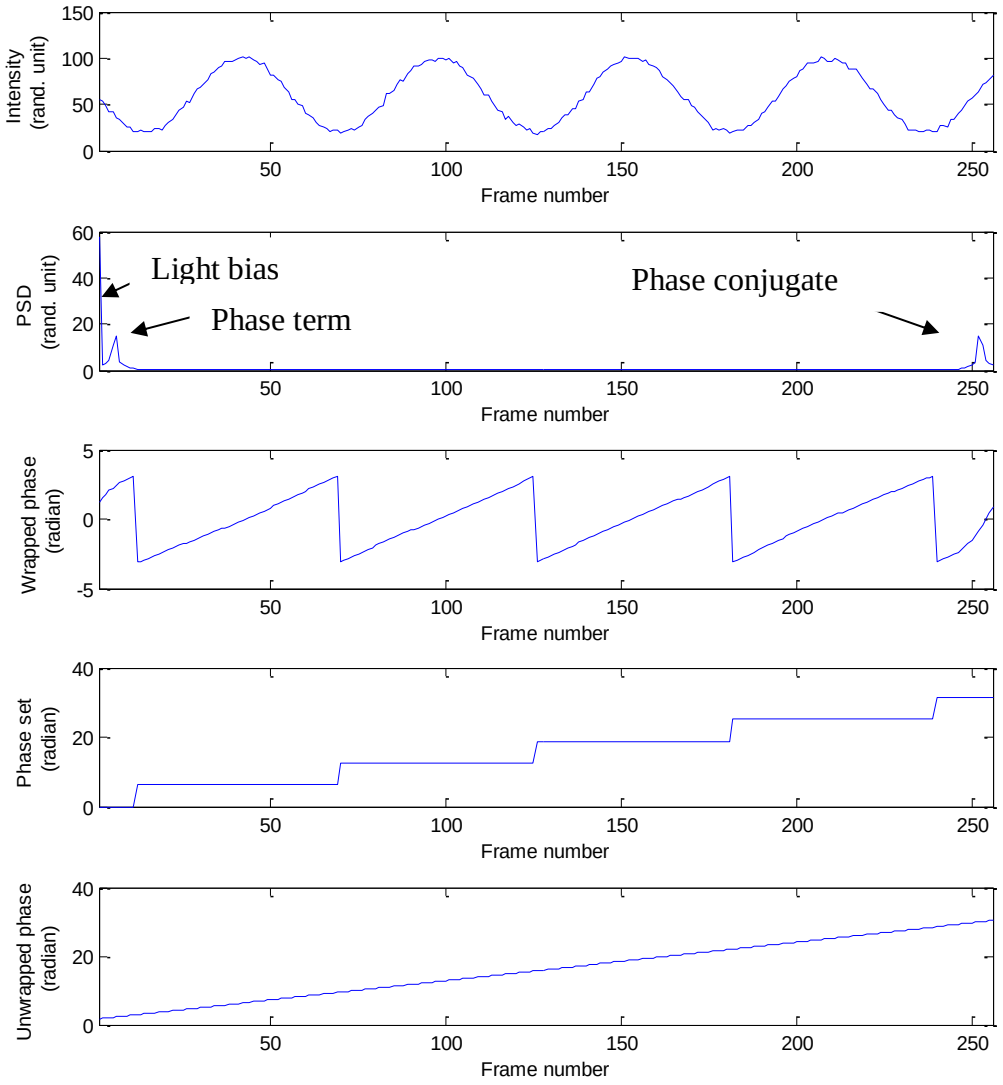

Fig. 2.2. Demonstration of the Takeda technique

Figure 2.3 shows how the interferometer output changes depending on the surface height. Since distance h_1 is less than h_2 with respect to the virtual reference plane, the fundamental frequency will be lower. Since the number of frames is the same in both cases there will be more data points per cycle at h_1. This gives better results when using Fourier phase slope method.

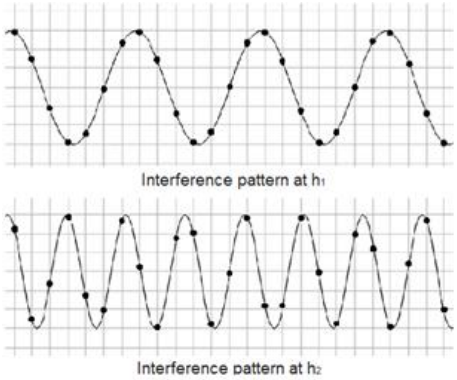

Fig. 2.3. Relationship between interference pattern and sampling points at different axial positions

WSI is effectively a frequency estimation problem, given that the position of each point on the measurand is determined by the rate of change of phase of the WSI interferogram. Techniques that rely on Fourier transforms, such as simple FFT and the Takeda method are limited in terms of the axial resolution that can be achieved and the consistency of resolution respectively.

There are alternative ways to estimate frequency without using Fourier transforms. Parametric methods model the WSI output as a stationary process, where a set of parameters describe the spectral density. The peak of the PSD function can thus be evaluated from this set of parameters corresponding to the sinusoidal output from the WSI wavelength scanning. When the PSD is estimated using parametric methods, a short data length does not necessarily result in a degradation of spectral resolution. This provides a key benefit in comparison to Fourier methods in relation to WSI as the data length can be limited by the scanning range or step resolution provided by the light source. Using a shorter wavelength sweep range without causing a degradation in resolution also means that measurement time could potentially be reduced by using parametric estimation methods.

3. Measurement algorithms for wavelength scanning interferometry

3.1.1. Introduction

WSI generates a set of spectral interferograms, where each pixel corresponds to a point of the surface being measured. At each pixel a sinusoidal intensity pattern is recorded corresponding to the scanning of the wavelength during measurement. The height of the surface at each point is then determined by calculating the amount of phase during the wavelength scan.

3.2. Optimised Height Determination Algorithms

There are various different methods that can be used to calculate the phase. At present Fourier transform methods are the most common, which are non-parametric i.e. they estimate the phase without assuming that the data has any particular structure. A fast Fourier transform (FFT) can be used to find the power spectral density (PSD) of the sinusoidal interference pattern and determine its frequency. Each cycle of the pattern represents a 2π phase shift so the phase shift can be found by multiplying the number of cycles by 2π.

An alternative way to calculate the PSD uses parametric estimation methods. These methods are based on a model of the data which assumes an underlying structure that can be described by certain parameters. If the parameters of the model can be estimated the PSD can be estimated from the frequency response of the model. These methods can provide a more accurate estimate in some circumstances as the resolution does not

necessarily reduce rapidly with decreasing normalised frequency, as it does with Fourier methods.

One type of model that can be used is an autoregressive (AR) model. These can give a more accurate spectral estimate with greater frequency resolution for short data records. They do not suffer from the leakage effects of windows because they use linear prediction to extrapolate the signal outside of its known values.

An autoregressive (AR) model predicts the output of a system based on previous outputs. An AR model is defined as

$$x_t = \sum_{i=1}^{p} a_i \, x_{t-i} \; + \; \varepsilon_t \tag{3.1}$$

where a_i are the AR coefficients, p is the model order, and ε_t is noise.

The PSD estimate using an AR model is given by

$$\hat{P}_{AR}(f) = \frac{\varepsilon_p}{\left|1 + \sum_{k=1}^{p} a_p(k) e^{-2\pi jkf}\right|^2} \tag{3.2}$$

3.2.1. Yule-Walker equations

To estimate the PSD we need to estimate the AR coefficients $\{a_1, a_2, \ldots a_p\}$. This can be done using the Yule Walker equations, which give the relationship between the AR parameters and the autocorrelation function of x_t.

For the general case AR(p), we multiply the equation by x_{t-k} (Chen et al, 2011)

$$x_{t-k} x_t = \sum_{i=1}^{p} (a_i x_{t-k} \, x_{t-i}) \; + \; x_{t-k} \varepsilon_t \tag{3.3}$$

and take the expectance

$$\langle x_{t-k} x_t \rangle = \sum_{i=1}^{p} (a_i \langle x_{t-k} x_{t-i} \rangle) + \langle x_{t-k} \varepsilon_t \rangle \tag{3.4}$$

$\langle x_{t-k} \varepsilon_t \rangle = 0$ for all $k > 0$ because the noise at the current time is not related to previous values of the process. So for $k \neq 0$, using the autocovariance function at lag k, $\gamma_k = \langle x_0 x_k \rangle$ we have

$$\gamma_k = \sum_{i=1}^{p} a_i \gamma_{k-i} \tag{3.5}$$

dividing through by γ_0 gives the autocorrelation coefficients R_k

$$R_k = \sum_{i=1}^{p} a_i R_{k-i} \tag{3.6}$$

This can be represented as a matrix

$$\begin{pmatrix} R_1 \\ R_2 \\ R_3 \\ \vdots \\ R_p \end{pmatrix} = \begin{pmatrix} R_0 & R_{-1} & R_{-2} & \dots & R_{-(p-1)} \\ R_1 & R_0 & R_{-1} & \dots & R_{-(p-2)} \\ R_2 & R_1 & R_0 & \dots & R_{-(p-3)} \\ \vdots & \vdots & \vdots & \ddots & \vdots \\ R_{p-1} & R_{p-2} & R_{p-3} & \dots & R_0 \end{pmatrix} \begin{pmatrix} a_1 \\ a_2 \\ a_3 \\ \vdots \\ a_p \end{pmatrix} \tag{3.7}$$

For $k = 0$ we have

$$R_0 = \sum_{i=1}^{p} a_i R_{-i} + \sigma_\varepsilon^2 \tag{3.8}$$

where σ_ε^2 is the standard deviation of the input noise.

Alternatively these can be combined and expressed as

$$\begin{pmatrix} \sigma_\varepsilon^2 \\ 0 \\ 0 \\ \vdots \\ 0 \end{pmatrix} = \begin{pmatrix} R_0 & R_{-1} & R_{-2} & \dots & R_{-(p)} \\ R_1 & R_0 & R_{-1} & \dots & R_{-(p-1)} \\ R_2 & R_1 & R_0 & \dots & R_{-(p-2)} \\ \vdots & \vdots & \vdots & \ddots & \vdots \\ R_p & R_{p-1} & R_{p-2} & \dots & R_0 \end{pmatrix} \begin{pmatrix} 1 \\ a_1 \\ a_2 \\ \vdots \\ a_p \end{pmatrix} \tag{3.9}$$

To determine the AR parameters the autocorrelation matrix must be solved with the $p+1$ estimated autocorrelation lags $R_0, R_1, \ldots, R_p$. Since it is a Toeplitz matrix this can be done with the Levinson-Durbin recursion. The algorithm proceeds recursively to compute the parameter sets $\{a_{11},\ \sigma_{\varepsilon 1}^2\}$, $\{a_{21},\ a_{22}\sigma_{\varepsilon 2}^2\}$, …, $\{a_{p1}, a_{p2}, \ldots, a_{pp}, \sigma_{\varepsilon p}^2\}$ where the additional subscript denotes the order. The final set at order p is the solution.

The solution to the first order predictor is given by

$$a_{11} = -R_1/R_0 \tag{3.10}$$

$$\sigma_1^2 = (1 - |a_{11}|^2)R_0$$

then the second order predictor

$$a_{21}R_0 + a_{22}R_1 = -R_1 \tag{3.11}$$

$$a_{21}R_1 + a_{22}R_0 = -R_2$$

combining the first and second orders to eliminate R_1 we get

$$a_{22} = \frac{a_{11}R_1 + R_2}{(1 - |a_{11}|^2)R_0} = \frac{a_{11}R_1 + R_2}{\sigma_1^2} \tag{3.12}$$

$$a_{21} = a_{11} + a_{22}a_{11}^*$$

and for the k^{th} order

$$a_{kk} = \frac{\sum_{l=1}^{k-1} a_{k-1.l}R_{k-1} + R_k}{\sigma_{k-1}^2} \tag{3.13}$$

$$a_{ki} = a_{k-1,i} + a_{kk}a_{k-1,k-i}^*$$

3.2.2. The Burg Method

The Burg method is another way to estimate the AR coefficients. It works by minimising sums of squares of forward and backward linear prediction errors with respect to the coefficients (Roth, Esquef & Valimaki, 2003). From the definition of an AR model

$$x_t = \sum_{i=1}^{p} a_i \, x_{t-i} \; + \; \varepsilon_t \tag{3.14}$$

it can be seen that the residual ε_t can be calculated from the signal x_t by (Kay & Marple, 1981)

$$\varepsilon_t = \; x_t + \sum_{i=1}^{p} a_i \, x_{t-i} = \sum_{i=0}^{p} a_i \, x_{t-i} \tag{3.15}$$

where $a_0 = 1$. A set of t values $\{x_0, x_1, \dots, x_{t-1}\}$ representing samples of a discrete-time signal can be approximated using coefficients $\{a_1, a_2, \dots, a_k\}$ by the forward linear prediction

$$f_n^{(l)} = -\sum_{i=1}^{l} a_i x_{t-1} \tag{3.16}$$

and by backward linear prediction

$$b_n^{(l)} = -\sum_{i=1}^{l} a_i x_{t+1} \tag{3.17}$$

The residual ε_p, ε_{p+1}, …, ε_{t-1} is considered to be the output of a finite impulse response (FIR) prediction error filter that can be implemented through a lattice structure with equations

$$\begin{aligned} f_n^{(l)} &= f_n^{(l-1)} + k_l b_{n-1}^{(l-1)} \\ b_n^{(l)} &= b_{n-1}^{(l-1)} + k_l f_n^{(l-1)} \\ n &= l, l+1, \dots, t-1 \end{aligned} \tag{3.18}$$

where k_l are the reflection coefficients of the stage l. The initial values for the residuals are $f_n^{(0)} = b_n^{(0)} = x_t$. The sum of residual energies in stage l is

$$E_l = \sum_{n=l}^{t-1} \left(f_n^{(l)}\right)^2 + \left(b_n^{(l)}\right)^2 \tag{3.19}$$

To estimate the AR coefficients we minimise E_l with respect to k_l

$$2\sum_{n=1}^{N-1} \left\{\left(f_n^{(l-1)} + k_l b_{n-1}^{(l-1)}\right) b_{n-1}^{(l-1)} + \left(b_{n-1}^{(l-1)} + k_l f_n^{(l-1)}\right) f_n^{(l-1)}\right\} \tag{3.20}$$

$$= 0$$

$$k_l = \frac{-2\sum_{n=1}^{N-1} f_n^{(l-1)} b_{n-1}^{(l-1)}}{\sum_{n=1}^{N-1}\left(f_n^{(l-1)}\right)^2 + \left(b_n^{(l-1)}\right)^2}$$

The AR coefficients a_k can then be retrieved from the reflection coefficients using the Levinson-Durbin algorithm described above. The recursion is initialised with $a_0 = 1$ and

$$a_m^{(l-1)} + k_l a_{l-m}^{(l-1)} \tag{3.21}$$

$$a_l^{(l)} = k_l$$

$$m = 1, 2, \ldots, l-1$$

and is repeated for $l = 1, 2, \ldots, p$.

3.3. Comparison of Yule Walker, Burg and non-parametric methods

Figure 3.1 shows a comparison between the resolving power of the AR methods Yule Walker and Burg compared to a periodogram. With short data records like this one it can be seen that the Burg method has the best resolving power. The Burg method also ensures a stable AR model, which the Yule Walker method does not, and is relatively

computationally efficient. However the Burg method can exhibit the problem of spectral line splitting.

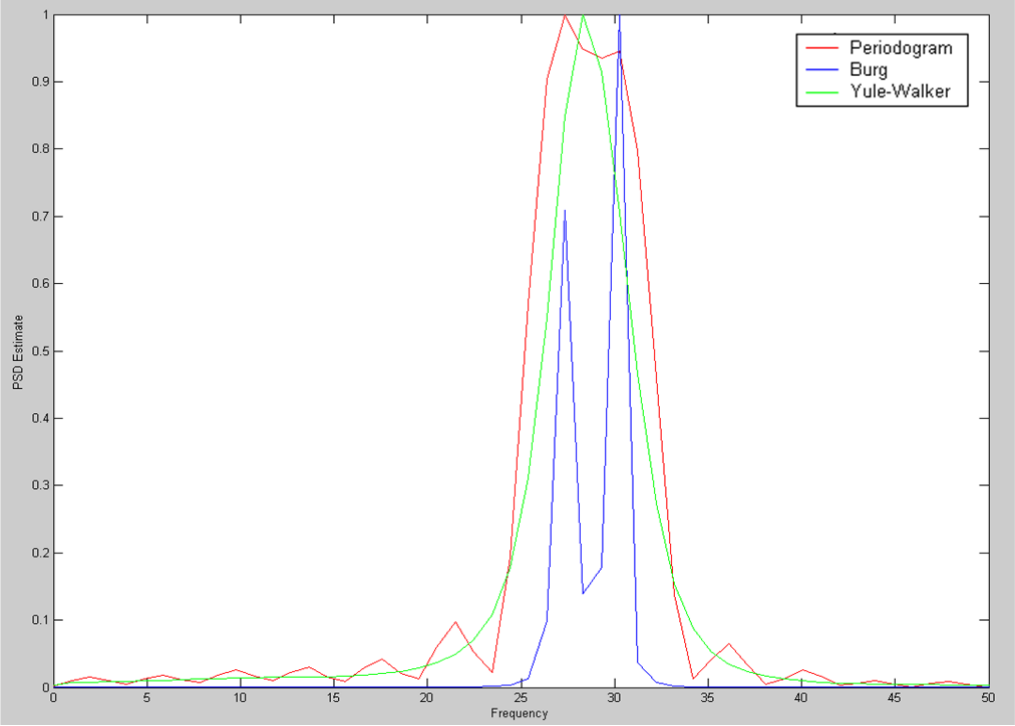

Fig. 3.1. Comparison of PSD estimates of a signal made up of two sinusoidal waves with frequencies of 27.5 and 30 with some Gaussian noise and sampled at 256 points

Table 3.1 shows the difference in resolving power between the Burg method and the periodogram (normalised frequency). From this it can be seen that the Burg method has improved resolution, especially for the shorted data records.

Table 3.1 Comparison of resolution for periodogram and Burg algorithms

Data records	**64**	**128**	**256**
Periodogram resolution	0.011	0.006	0.003
Burg resolution	0.005	0.003	0.002

Figure 3.2 shows a comparison between the PSD estimates produced by the periodogram and Burg methods with different lengths of data record. It can be seen clearly how the periodogram resolution decreases with decreasing record length as the full width at half maximum (FWHM) of the peaks increases. In contrast, for the Burg method the FWHM does not depend as heavily on the length of the data record, allowing for better resolution with fewer data points.

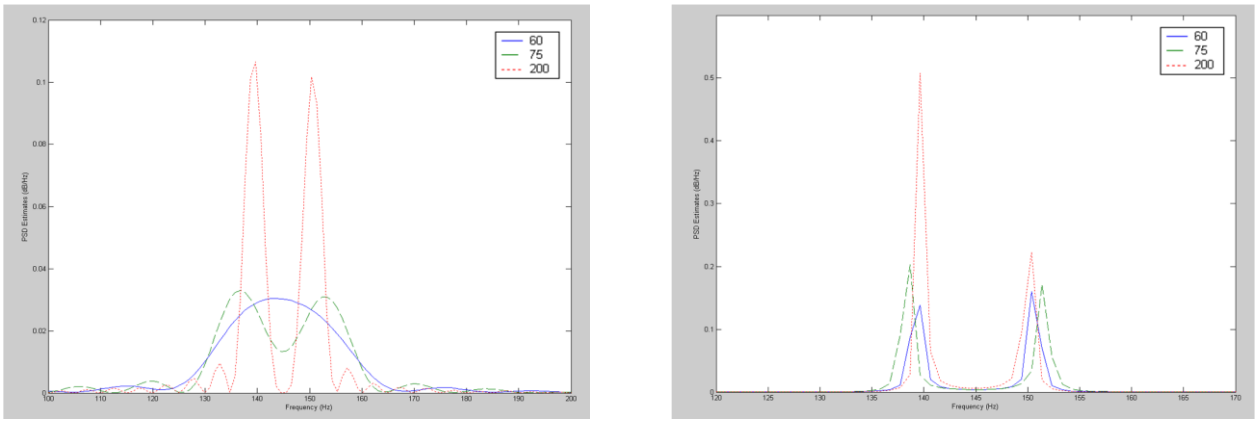

(a) (b)

Fig. 3.2. Comparison of PSD estimates produced by a periodogram (a) and the Burg method (b) of a signal made up of two sinusoidal waves with frequencies of 140 and 150 with 60, 75 and 200 data points.

3.4. The Tapered Burg Algorithm

Although the Burg method provides more consistent resolution at different surface heights than the Fourier phase slope method, it also suffers from additional problems. In particular, for short data records, there are frequency errors that depend on the phase of sinusoidal components of a signal and spectral line splitting can occur, particularly when there is a

high signal-to-noise ratio. The effect of these problems can be reduced by modifying the algorithm.

One such modification is to replace the rectangular taper used in the original Burg method with a taper is calculated to minimise the frequency error across all phases (Roth, Esquef & Valimaki, 2003). The modified algorithm works by "tapering" the original Burg algorithm using a calculation of the frequency error produced when the Burg method is applied to a sinusoid.

Swingler (1980) showed that the estimated frequency error for a sinusoid $x_k = \cos(k\theta + \phi)$, $k = 0,1,\dots,N$ is given by the expression

$$\Delta f = \frac{1}{N}\cos(N\theta + 2\phi)\frac{\sin(N\theta)}{\sin(\theta)} \tag{3.22}$$

If the phase is considered to be a random uniformly distributed variable then the mean frequency error is zero and the variance is (Roth, Esquef & Valimaki, 2003)

$$\mathrm{var}(\Delta f) = \frac{1}{8\pi^2}\sin^2(\theta)\sum_{k=0}^{N-1}\sum_{l=0}^{N-1} w_{1,k}, w_{1,l}\cos\big(2\theta(k-l)\big) \tag{3.23}$$

The taper is the chosen to minimise the average frequency error variance with respect to the taper.

3.5. Comparison of Burg and Tapered Burg Methods

In order to compare the results produced by the Burg method and the tapered Burg method, a numerical simulation of the determination of a sinusoidal frequency from an interferogram produced by WSI was carried out. A sinusoid sample at 256 points and with a normalised frequency of 0.1083 was used as an input. This data length corresponds to the number of interferograms captured by the WSI in the experimental data. The normalised frequency corresponds to an axial position of 30 μm from the virtual reference.

Using normalised frequency to assess the performance of the algortithms in general terms means that results can easily be applied to other apparatuses. Additive Gaussian white noise (AGWN) was added to the simulated sinusoid. The signal-to-noise ratios (SNR), defined by the ratio of the mean signal and the standard deviation of the AGWN, was 58.2 dB which corresponds to typical values found from experimenal data. Figure 3.3(a) shows the PSDs calculated using the Burg algorithm for 3 independent runs. It appears that the PSD peak in each case varies significantly due to the applied noise, which will create a problem if this algothim is used for WSI estimation. Figure 3.3(b) shows the same datasets processed using the tapered Burg algorithm, where stable results are produced across all 3 runs.

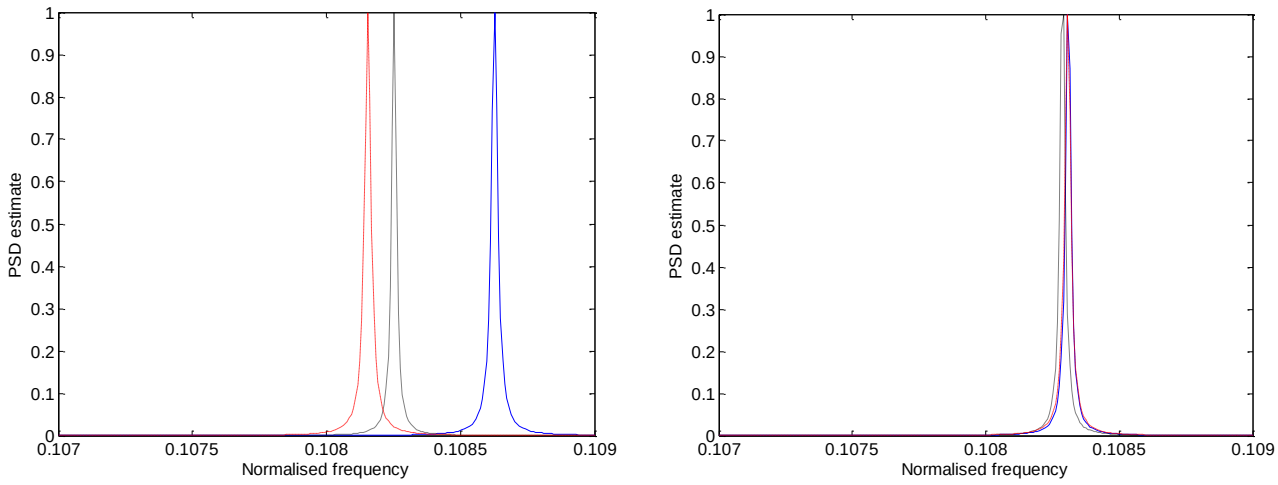

Fig. 3.3. Comparison of PSD estimates produced by the (a) Burg method and (b) tapered Burg method

Since the tapered Burg method is established as the most stable in terms of resolving spectral interferogram frequency, the study was then extended to look at how the algorithm performs when used at various axial positions with respect to the VRP.

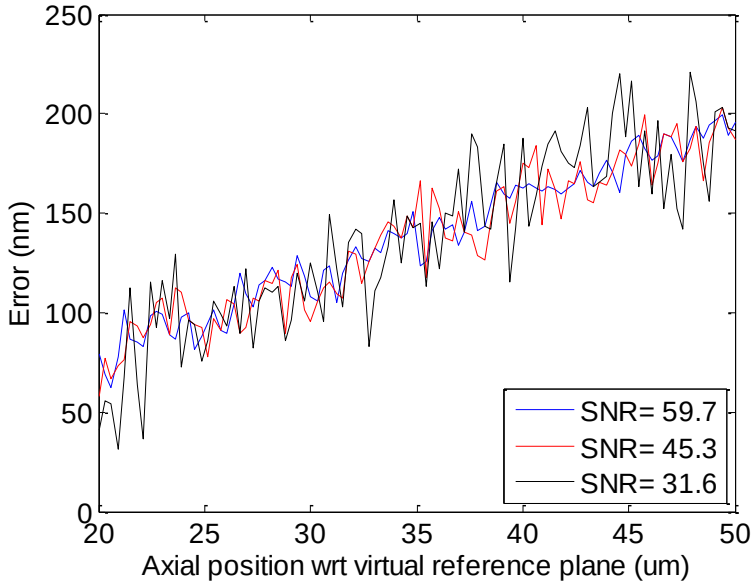

Fig. 3.4. Simulated measurement error with axial position and SNR

Figure 3.4 shows the error in frequency estimation, which has been converted to the corresponding axial position error, as the axial position with respect to the VRP is moved in 100 increments between 20 to 50 µm (equivalent to a normalised frequency range of 0.072 to 0.180 for our apparatus). The tests were repeated 3 times, in each case the amplitude of AGWN was doubled, which created an SNR of 31.6 dB, 45.3 dB and 59.7 dB for the respective runs. From the results an overall trend of the error in frequency estimation increasing as the axial position moves away from the VRP (increasing normalised frequency) can be seen. Reducing the SNR does not appear to have a significant effect on the ability of the tapered Burg method to resolve the interferogram frequency.

3.6. Comparison of the Burg methods with Fourier techniques

In order to evaluate any benefits in performance that can be attributed to the use of an auto-regressive model based frequency estimation technique for WSI a comparison was made to the performance of the currently used Fourier based methods. A numerical simulation

was performed where the axial position with respect to the VPR was moved over 100 increments between 20 and 50 µm. The results of this simulation are shown in Figure 3.5. For the simple FFT there is a large cyclic error which results from the discretisation of the frequency estimation. This can to some degree be counteracted by using interpolation techniques. It can be seen that the Takeda method, which is based on phase gradient estimation, exhibits the best performance in terms of error in frequency estimation, but beyond 41 µm it starts to diverge and the technique effectively becomes unusable . The tapered Burg exhibits a slightly higher estimation error when compared to the Takeda method but on the other hand the results are still usable across the entire investigated range. This suggests that the tapered Burg estimation method has the potential to be used to increase the measurement range of WSI systems without altering aspects of the physical apparatus such as depth-of-field and coherence length.

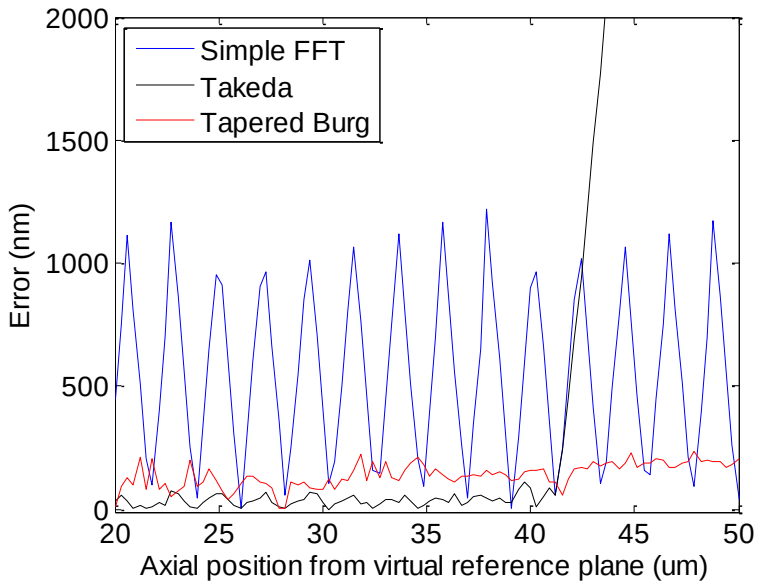

Fig. 3.5. Comparison of Fourier and AR model based methods of frequency determination in WSI

In order to validate the simulated results by comparing them to real data, the WSI apparatus shown in Figure 2.1 was used to measure a small step height at two axial positions: 30 µm and 50 µm with respect to the VRP. The measurand used was an etched waffle plate sample with a nominal well depth of 100 nm. An areal measurement of individual well was undertaken for this study, the stated axial position corresponds to the position of the upper face of the plate. To conduct the measurements, the sample was placed on a precision translation stage so that the axial position could easily be adjusted. The measurement consisted of 256 interferograms taken between a source wavelength range of 590.98 nm and 683.42 nm using a x5 magnification objective.

Figure 3.6 (a) and (b) shows the results from the areal measurements where the spectral interferograms have been processed using the Takeda method. The measurements appear to be well resolved where the upper face is located 30 µm from the VRP. However, when the upper face is placed at 50 µm from the VRP the algorithm becomes unstable and the results produced are invalid.

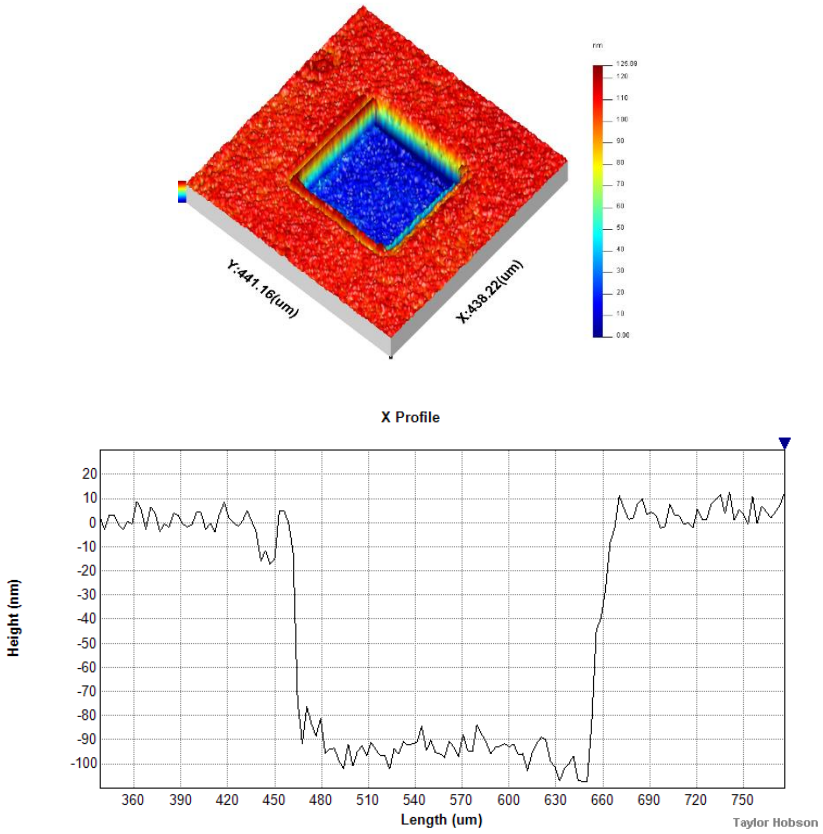
Y:441.16(um)
X:438.22(um)
X Profile
Height (nm)
Length (um)
Taylor Hobson

(a)

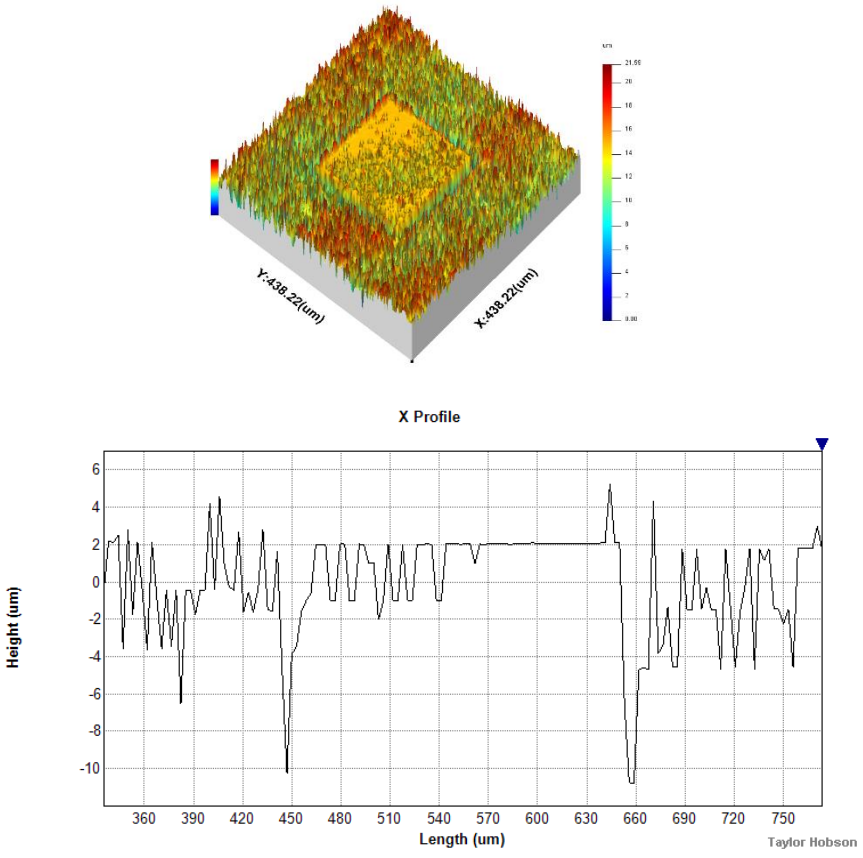
Y:438.22(um)
X:438.22(um)
X Profile
Height (um)
Length (um)
Taylor Hobson

(b)

Fig. 3.6. Waffle plate surface topograph as evaluated by the Takeda method at axial positions of (a) 30 µm and (b) 50 µm

The tapered Burg algorithm was then used to process the same datasets as described above. Figure 3.7 shows that this algorithm is able to successfully resolve the data with the axial positions at both 30 µm and 50 µm. This corroborates the simulated data and validates the use of AR model based methods for extending the WSI measurement range. Comparing Figure 3.6(a) and 3.7(a), there appears to be less measurement noise associated with the Takeda method than the tapered Burg, which correlates with the error plots comparison shown in Figure 5.

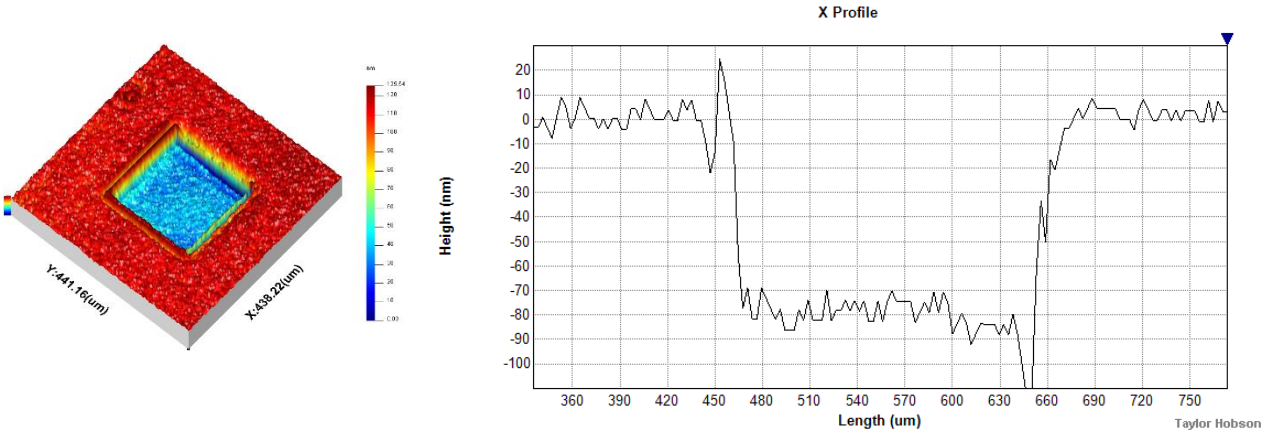

(a)

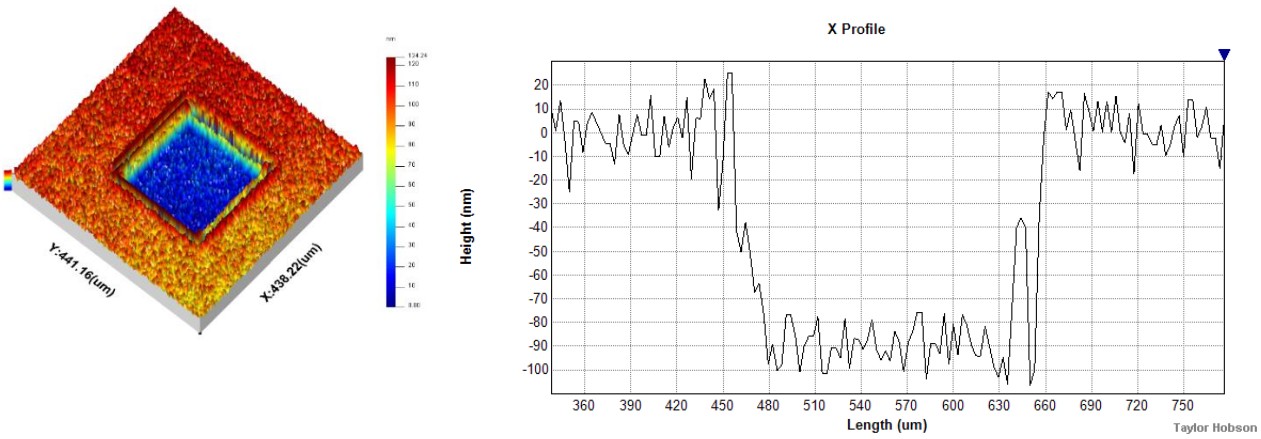

(b)

Fig. 3.7. Waffle plate surface topograph as evaluated by the tapered Burg method at axial positions (a) 30 µm and (b) 50 µm

3.7. Conclusion

These results show that auto-regressive frequency estimation techniques, in particular the tapered-window variant of the Burg algorithm, are able to improve measurement performance in WSI for some applications. The tapered Burg algorithm was able to resolve surface features across a wider range of axial positions compared to current algorithms, effectively demonstrating an extended measurement range.

4. Discussion, conclusions and future work

4.1. Discussion

Wavelength scanning interferometry is a next-generation optical measurement system that can be used to provide areal characterisations of complex surfaces. The resolution of the surface height measurement using WSI depends on the accuracy of the algorithm used to evaluate the phase shift obtained from the wavelength scanning process. Fourier transform methods are the most commonly used phase estimation technique at present, but they can experience problems in some circumstances, for example when dealing with short data records. Parametric methods such as the Burg method have the potential to provide improved results in some cases.

The Burg method is a way of estimating the autoregressive coefficients to provide a PSD estimate from an autoregressive model. The original Burg method uses a rectangular taper, but this can lead to frequency errors and spectral line splitting, particularly when there is a high signal-to-noise ratio. A modified algorithm works by tapering the original Burg algorithm using a calculation for the frequency error the algorithm produces for a sinusoid to minimise the frequency error across all phases.

4.2. Conclusions

A simulation of the WSI output was used to compare the performance of the Burg method and non-parametric methods. Table 3.1 compares the resolving power of Burg method and the periodogram (normalised frequency), showing that that the Burg method has improved resolution, especially for the shorted data records.

A 100 nm well feature from an etched waffle plate artefact was measured. 256 interferograms were taken between a source wavelength range of 590.98 nm and 683.42 nm using a x5 magnification objective. The measurements taken at 30 µm as seen in Figure 3.6 (a) show good results for the Takeda method and there appears to be less measurement noise compared to the tapered Burg method in Figure 3.7 (a). However the tapered Burg algorithm was able to resolve the well structure across a wider range of axial positions, effectively demonstrating an extended measurement range. This can be seen from the results of the 50 µm measurement in Figure 3.7 (b). At 50 µm the Takeda algorithm is not able to resolve the feature as the algorithm becomes unstable as seen in Figure 3.6 (b).

4.3. Contribution

- The introduction of the Burg algorithm as a method to calculate the surface height from WSI output.
- The demonstration of an extended measurement range of 50 µm using the tapered Burg algorithm in comparison to 30 µm with current Fourier techniques.
- The publication of a paper "Burg algorithm for enhancing measurement performance in wavelength scanning interferometry".

4.4. Future work

Further work in this area will establish the potential for improving measurement performance in WSI by applying auto-regressive model based techniques. Improvements can be made by focusing on the analysis of measurement uncertainty, reduction of algorithm-related measurement noise and computation time.

5. References

Carnahan, E.G.B.a.J.W., *Characterization of an Acousto-optic Tunable Filter and Use in Visible Spectrophotometry.* Applied Spectroscopy, 1999. **53**(5): p. 603-611.

Chen, W., et al., *Solutions of Yule-Walker equations for singular AR processes.* Journal of Time Series Analysis, 2011. **32**(5): p. 531-538.

Jiang, X., Wang, Kaiwei, Gao, F. & Muhamedsalih, Hussam, *Fast surface measurement using wavelength scanning interferometry with compensation of environmental noise.* 2010(Journal Article).

Jiang, X., Scott, Paul J., Whitehouse, D.J. and Blunt, Liam, *Paradigm shifts in surface metrology. Part II. The current shift*. Proceedings of the Royal Society A: Mathematical, Physical and Engineering Science, 2007. 463(2085): p. 2071-2099.

Kay, S.M. and S.L. Marple, *Spectrum analysis-A modern perspective.* Proceedings of the IEEE, 1981. **69**(11): p. 1380-1419.

Kikuta, H., Iwata, K., and Nagata, R., *Distance measurement by the wavelength shift of laser diode light*, Appl. Opt. 25, 2976-2980, 1986.

Kuwamura, S and Yamaguchi, I, *Wavelength scanning profilometry for real-time surface shape measurement*, Appl. Opt. 36, 4473-4482, 1997.

Roth, K, Esquef, P and Valimaki, V, *Frequency warped Burg's method for ARmodeling.* Proc. IEEE, 2003: p. 5-8.

Swingler, D., *Frequency errors in MEM processing. Acoustics, Speech and Signal Processing*, IEEE Transactions on, 28(2), 257-259 (1980).

Suematsu, Masakazu, and Takeda, Mitsuo, "*Wavelength-shift interferometry for distance measurements using the Fourier transform technique for fringe analysis*," Appl. Opt. 30, 4046-4055, 1991.

Takeda, M & Yamamoto, *Fourier-transform speckle profilometry: threedimensional shape measurements of diffuse objects with large height steps and/or spatially isolated surfaces*. Applied Optics, 33 7829-7837, 1994.